Ultra-wideband Antenna System Design for Future mmWave Applications

Muhannad Y. Muhsin[1], Zainab S. Muqdad[2], Asaad H. Sahar[3], Zainab F. Mohammad[1],
and Hussam AL-Saedi[1]

[1] *University of Technology – Iraq, Baghdad, Iraq,*
[2] *Mustansiriyah University, Baghdad, Iraq,*
[3] *University of Baghdad, Baghdad, Iraq*

https://doi.org/10.26636/jtit.2025.1.1951

Abstract — An ultra-wideband planar four-element multiple-input multiple-output (MIMO) antenna array for millimeter wave (mmWave) 5G applications is presented in this article, characterized by a simple structure and diverse performance capabilities. The antenna system operates in the 20 GHz band (ranging from 42.3 to 63.3 GHz), with a high gain of 7.8 dB. The compact size of 25 × 25 mm makes it suitable for being integrated with various telecommunication devices used in a number of mmWave applications. The antenna's elements are placed orthogonally, achieving great isolation of over 24 dB. The performance of the proposed antenna was analyzed in terms of its s parameters, gain, efficiency, radiation patterns, and MIMO diversity characteristics, including the envelope correlation coefficient (ECC), diversity gain (DG), and mean effective gain (MEG).

Keywords — 5G, antenna array, mmWave, UWB

1. Introduction

Fifth-generation communication networks represent a substantial advancement in wireless technologies, providing considerable potential for high-speed data transmission and ultralow latency [1]–[3]. The mmWave spectrum provides extensive capacity, allowing data rates to surpass those of former cellular networks [4]. The MIMO communication technology is used at high frequencies to achieve such a high data rate. In light of the above, it is necessary to design a system of MIMO antennas that relies on multiplexing technologies and spatial diversity to improve reliability, data throughput and coverage [5], [6].

Researchers aim to improve various antenna performance parameters, including bandwidth, compactness, efficiency, gain, and diversity characteristics. Many techniques are deployed to optimize performance, including substrate selection, dielectric lens, multi-element configurations, corrugation, and mutual coupling reduction [7], [8].

The substrate utilized in the design of each antenna is of key significance. A substrate with reduced relative permittivity and lower loss tangent will enhance gain while minimizing power losses [9]. A corrugated construction, which eliminates the metallic part of the edge radiator, is capable of improving the front-to-back ratio and the antenna's bandwidth [10]. Furthermore, the multi-element technique improves gain, efficiency, and bandwidth. Consequently, structures relying on the abovementioned solutions are capable of achieving elevated gain and bandwidth levels – a feature that one antenna only cannot offer. Moreover, a dielectric lens is capable of transmitting electrostatic radiation in a non-directional manner, thereby enhancing the antenna's directivity and gain, as shown in [11], [12].

Techniques relied upon to reduce mutual coupling decrease the impact that numerous elements exert on the system's performance. This method, referred to as an isolation technique, plays and important role in optimizing the performance of good diversity in MIMO structures [13], [14]. In addition, high gain is expected in mmWave antenna designs due to the increased free space path loss observed at these frequencies. Therefore, achieving decent performance of ultra-wideband MIMO antenna systems (in terms of high isolation and reasonable radiation characteristics) while maintaining their compact size and simple structure remains a challenge.

2. Related Works

In [15], a four-element MIMO array has been developed, where the antenna measuring only 30 × 35 × 0.76 mm. It operates at 25.5 – 29.6 GHz, with a gain of 8.3 dBi. The antenna design from [16] does not include decoupling surfaces and has a patch array. It offers a gain of 13.1 dBi within a frequency range of 26.94 – 31.08 GHz, with isolation below 14 dB.

In [17], the authors employed the DGS technique to provide robust isolation between an input port of the MIMO antenna array. In [18], a radiating element based on multiple arcs has been developed for mmWave MIMO applications, achieving a bandwidth of 23.5 – 38 GHz and offering a high isolation level of above 23 dB by arranging the radiating parts in an orthogonal configuration. Nevertheless, the overall profile of the antenna is rather large.

In [19], the researchers designed a tree-shaped antenna with multiple arcs to provide a wide broadband response of 23 – 40 GHz, an overall gain of 8 dBi and good isolation.

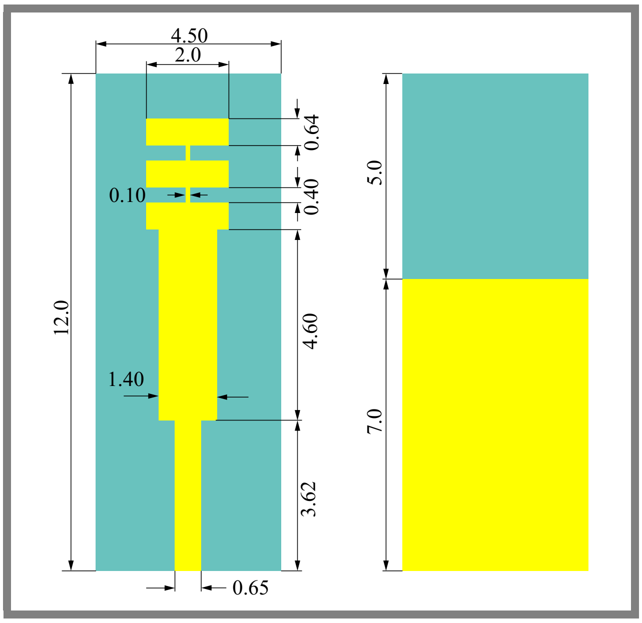

Fig. 1. Single antenna element: a) top view and b) back view.

A 4-element MIMO system designed for the 5G frequency spectrum of 27.5 – 40 GHz, with an entire dimension of 158 × 77.8 mm, was presented in [20], while paper [21] proposed an 8-port MIMO antenna array for the 27.5 – 29.5 GHz frequency range. In articles [22]–[25], metamaterial is used to achieve enhanced port isolation. A MIMO antenna array supporting 5G is presented in [26], achieving an array gain of 5 dB with a frequency band better than 26 – 39 GHz. In papers [27] and [28], another MIMO antenna array is proposed with high bandwidth and good radiation characteristics.

This article presents an ultra-wideband four-element MIMO array for mmWave applications featuring a simple structure and compact size of 25 × 25 mm. High isolation exceeding 24 dB is achieved thanks to orthogonal polarization diversity and excellent MIMO performance. It is a four-antenna MIMO system operating in the range of 42.3 to 63.3 GHz (20 GHz bandwidth). The antenna element is made up of two microstrip line steps (with different widths and lengths) and three symmetrical ladder steps located at the top. The proposed structure may be easily integrated with various devices used in mmWave applications. The CST Microwave Studio was used in the simulations.

3. Design

For micro-wave applications, printed antennas are optimal solutions due to their low profile, low cost, compact dimensions, as well as good balance between performance and manufacturing complexity. The proposed antenna utilizes the RT-5880 substrate, characterized by a loss tangent of 0.0009 and a relative permittivity of 2.2, with a thickness of 0.8 mm.

Figure 1 illustrates the shape and various parameters of the design. The size of the single antenna unit is 4.5 × 12 mm. The top view is presented in Fig. 1a, showing two microstrip line steps (with different widths and lengths) and three symmetrical ladder steps at the top of the antenna. The two-line steps have dimensions of 0.65 × 3.62 mm and 1.40 × 4.60 mm, respectively, while the symmetric ladder steps measure 2 × 0.64 mm. Figure 1b shows the back view of the antenna element with an etched ground plane.

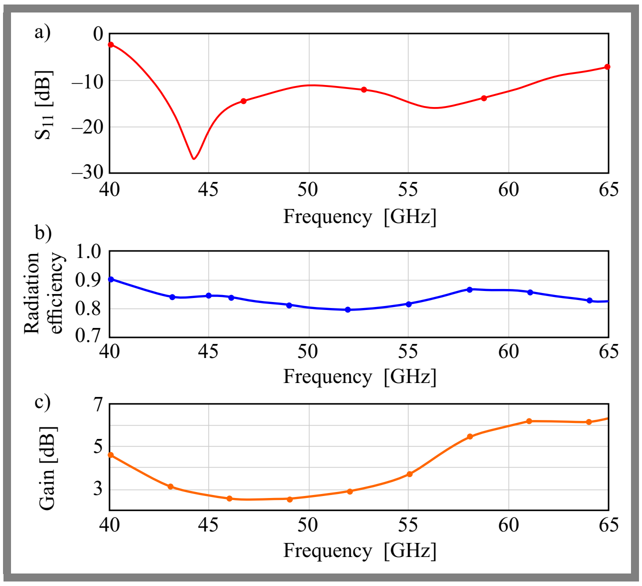

Fig. 2. a) S_{11} of the single antenna element, b) radiation efficiency, and c) gain.

The performance of a single antenna element is evaluated in terms of resonance frequency, bandwidth, radiation patterns, gain, and efficiency. Figure 2a illustrates the results of simulations of the reflection coefficient S_{11} versus frequency. It is clear that S_{11} remains below –10 dB across the entire frequency range of 42 to 62 GHz, i.e. ultra-wideband of 20 GHz with good impedance matching.

Figure 2b shows the radiation efficiency, which remains in the range of 80 – 88% within the entire working band. High antenna efficiency that remains stable within the ultra-wide working bandwidth is realized. The maximum gain reaches 6.2 dB, as can be observed in Fig. 2c. Such a high gain is required to eliminate the problem of propagating losses in

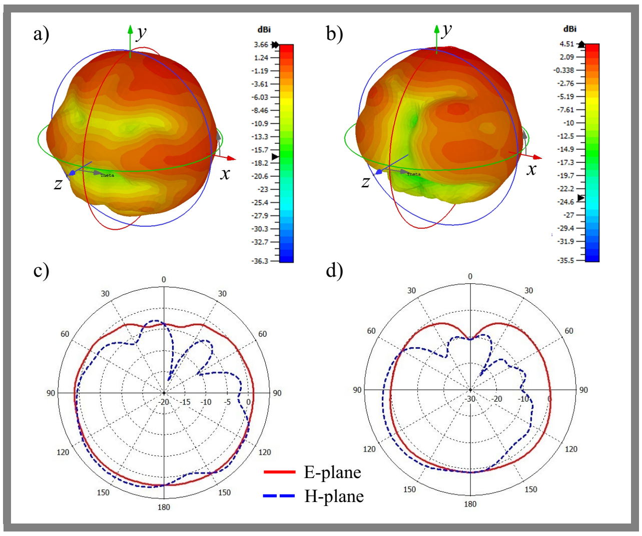

Fig. 3. 3D antenna radiation patterns at: a) 45 GHz, b) 55 GHz, and 2D antenna radiation patterns at: c) 45 GHz, d) 55 GHz.

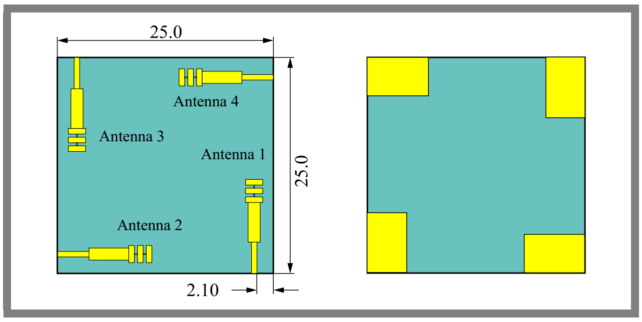

Fig. 4. Proposed antenna array system: a) top view and b) bottom view.

the mmWave spectrum. The radiation pattern for mmWave applications is visualized in Fig. 3. The three-dimensional radiation patterns at 45 GHz and 55 GHz are presented in Fig. 3a–b, while the E-plane and H-plane of the two-dimensional radiation patterns are illustrated in Fig. 3c–d.

4. Antenna Array System Design

Next, a four-element MIMO array is developed utilizing the single antenna described in Section 3. The MIMO elements are symmetrically and rotationally arranged in 90° intervals, creating a square configuration, as demonstrated in Fig. 4. Such a layout employs the polarization diversity approach used to minimize mutual coupling between the antennas. The dimensions of the MIMO system equal 25 × 25 mm.

Figure 5 illustrates the surface current distribution of the four-port MIMO antenna, where one port is excited and the other ports are connected to 50 Ω at the two frequencies of 45 GHz and 55 GHz, respectively. One may notice that the current flow is predominantly concentrated in the antenna unit with less propagation to other MIMO ports. The existence of multiple identical elements in a MIMO configuration results in an increase in mutual interference and ECC value between the antenna's elements. The orthogonal arrangement of the array results in the lowest possible mutual coupling.

Figure 6 shows the S-parameters for the proposed 4-element MIMO antenna design. All four return loss coefficients of the antennas are below –10 dB within the considered band of 20 from 42.3 to 62.3 GHz. This guarantees optimized impedance matching. Furthermore, a very slight variation can be observed between the return loss of the four elements and the single antenna element from Fig. 2. This proves a satisfactory mutual coupling between the antennas due to their structural similarity and the orthogonal MIMO layout. All transmission coefficients are lower than –24 dB (Fig. 6b), i.e., high isolation is obtained by applying the polarization diversity technique.

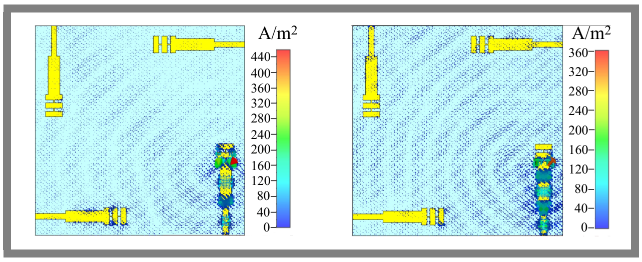

Fig. 5. Current distribution of the MIMO antenna array at: a) 45 GHz and b) 55 GHz.

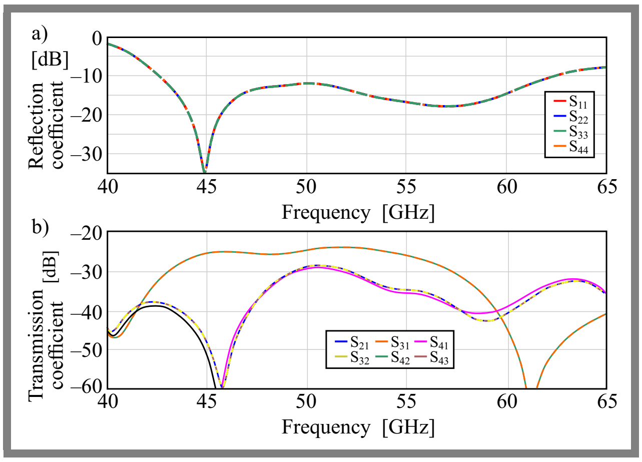

Fig. 6. S-parameters of the ultra-wideband quad MIMO antenna array: a) return loss and b) transmitting coefficients.

Figure 7a shows the radiation efficiency and total antenna efficiency of the designed MIMO elements. The total antenna efficiencies for the overall operating band remain within the 66 to 72% range, while the antenna's radiation efficiencies vary from 78 to 80%. Figure 7b illustrates the gain of the proposed MIMO antennas in its operating band. The gain of all antennas is in range of 4.1 to 7.8 dB.

Figure 8 presents the two-dimensional radiation patterns at the frequency of 45 GHz and 55 GHz, respectively. As demonstrated, the peak gain of the antennas is acieved in diverse directions, demonstrating the highly desired benefit of the patterns' diversity. Furthermore, these radiation patterns fully cover all sides, proving excellent radiation coverage.

Analysis of diversity parameters such as ECC, MEG, and DG is as essential evaluation of the antenna's key performance parameters, including bandwidth, radiation patterns, resonance

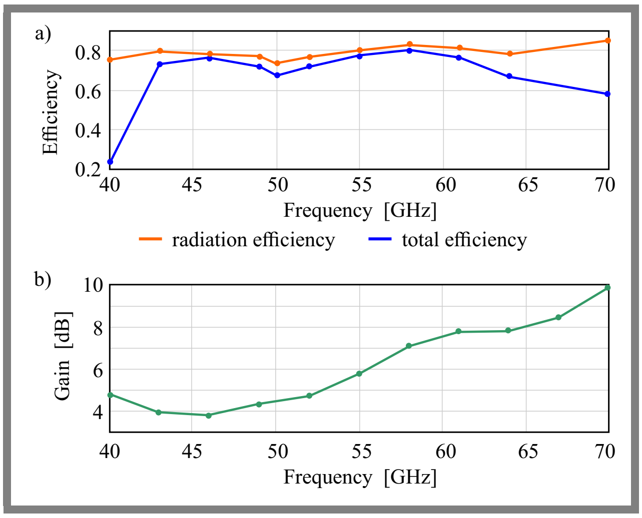

Fig. 7. Total and radiation efficiencies of the MIMO antenna array a) and gain b).

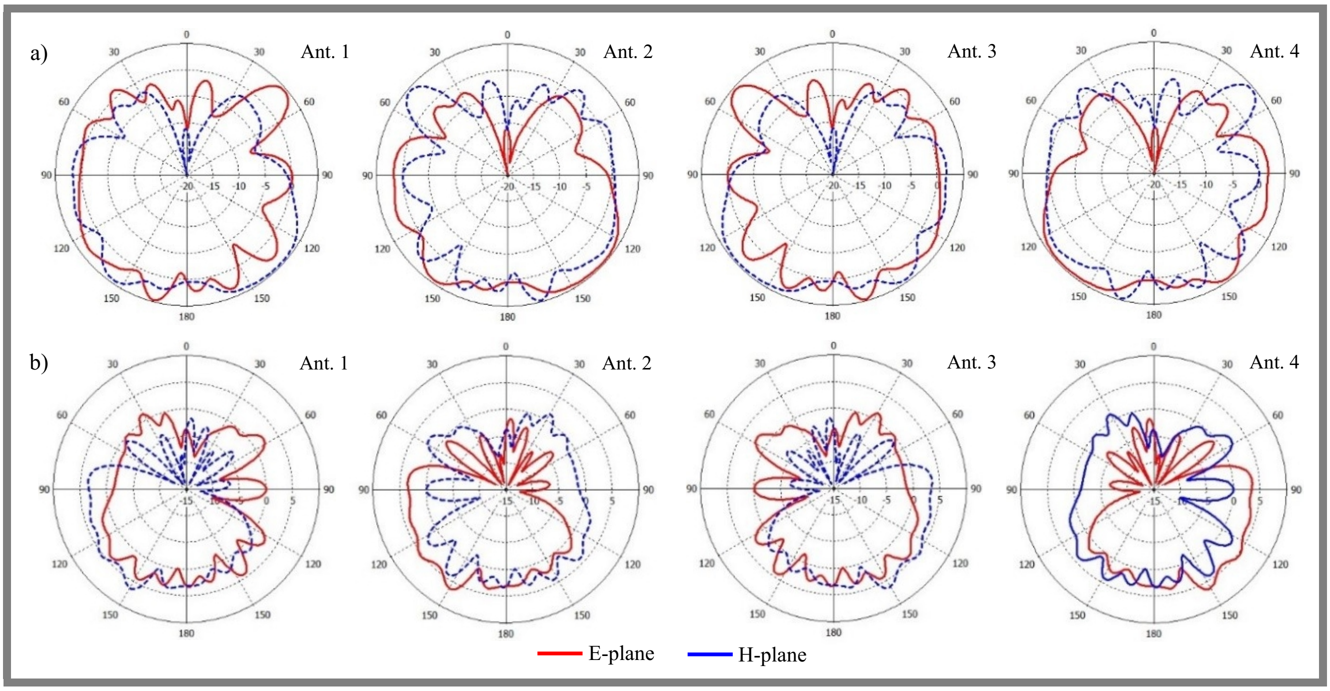

Fig. 8. 2D antenna radiation patterns at: a) 45 GHz and b) 55 GHz.

frequency, efficiency, and gain, as it allows to determine the efficacy of MIMO antenna arrays.

ECC determines the correlation between different antenna elements in a MIMO system. A low ECC value leads to less interdependence between the components and, hence, better MIMO diversity performance. Equations (1) and (2) illustrate how ECC is calculated using the scattering parameters and the far-field radiation pattern, respectively [13], [29].

$$ECC = |\rho_{ij}| = \frac{\left|S_{ii}^{*}S_{ij} + S_{ji}^{*}S_{jj}\right|^2}{\left(1-(|S_{ii}|^2+|S_{ji}|^2)\right)\left(1-(|S_{jj}|^2+|S_{ij}|^2)\right)}\,, \tag{1}$$

$$ECC = \frac{\left|\int\int_{4\pi}[\overrightarrow{F_1}(\theta,\varphi)^{*}\cdot\overrightarrow{F_2}(\theta,\varphi)]d\Omega\right|^2}{\int\int_{4\pi}\left|\overrightarrow{F_1}(\theta,\varphi)\right|^2 d\Omega\cdot\int\int_{4\pi}\left|\overrightarrow{F_2}(\theta,\varphi)\right|^2 d\Omega}\,, \tag{2}$$

where ρ_{ij} represents the envelope correlation coefficients (ECC) between the i and j antenna elements, $\overrightarrow{F_1}(\theta,\varphi)$ specifies 3D radiation pattern field with excitation at port i, $*$ signifies the Hermitian product and Ω indicates the solid angle.

In this work, the ECC from far field radiation patterns is taken into consideration. The expected ECC is less than 0.5, which falls within the permissible range for MIMO diversity. As illustrated in Fig. 9, very low ECCs are obtained, i.e. below 0.002, proving the very high diversity antenna system is achieved.

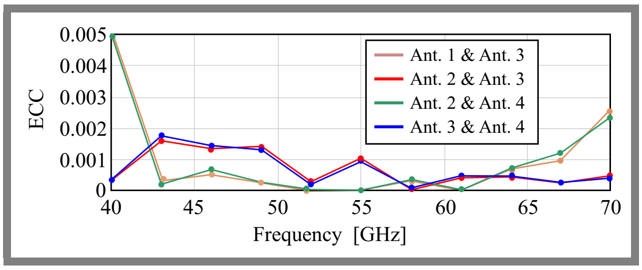

Fig. 9. ECCs of the proposed system.

The MEG is an other important performance criterion for MIMO systems, defined as the ratio of the mean received power to the total mean incident power at the antenna [30]. MEG quantifies the mutual interaction of antenna elements and the statistical characteristics of the propagation environment. Equations (3) and (4) illustrate the method of obtaining the MEG value from s parameters or far-field radiations. The MIMO antennas MEGs must satisfy the requirements of Eq. (5). The XPR indicates the cross polarization power ratio, while the gains of the antenna are described by G_θ and G_φ. The P_θ and P_φ are incoming plane waves components. The variables i and k in Eq. (4) denote the observed antenna and the total antennas number, respectively. The MEGs for the i and j antennas are designated as MEG_i and MEG_j, respectively.

$$MEG_i = 0.5\left(1-\sum_{j=1}^{k} S_{ij}\right)\,, \tag{3}$$

$$MEG = \int_0^{2\pi}\int_0^{\pi}\left(\frac{XPR}{1+XPR}G_\theta(\theta,\varphi)\,P_\theta(\theta,\varphi) + \frac{1}{1+XPR}G_\varphi(\theta,\varphi)\,P_\varphi(\theta,\varphi)\right)\sin\theta\,d\theta\,d\varphi\,, \tag{4}$$

$$\frac{MEG_i}{MEG_j} \cong 1\,. \tag{5}$$

Tab. 1. Comparison between the proposed MIMO array system and recent publications.

Ref.	Bandwidth [GHz]	Total efficiency [%]	Peak gain [dB]	Isolation [dB]	ECC	MIMO order	Overall size [mm]	Isolation technique
[15]	25.5 – 29.6	> 82	8.3	> 20	< 0.01	4 × 4	30 × 35	DGS
[20]	23 – 40	> 70	12	> 20	< 0.001	4 × 4	80 × 80	DGS
[32]	27.5 – 40	> 75	7.2	> 17	< 0.001	4 × 4	158 × 77.8	Spatial diversity and polarization diversity
[33]	20 – 32	80 – 90	6.5	> 20	< 0.001	4 × 4	24 × 32	Decoupling structure on ground plane
[34]	27 – 29	80 – 84	5.5	> 17	< 0.03	4 × 4	30 × 30	Polarization diversity
This work	42.3 – 63.3	66 – 72	7.8	> 24	< 0.002	4 × 4	25 × 25	Polarization diversity

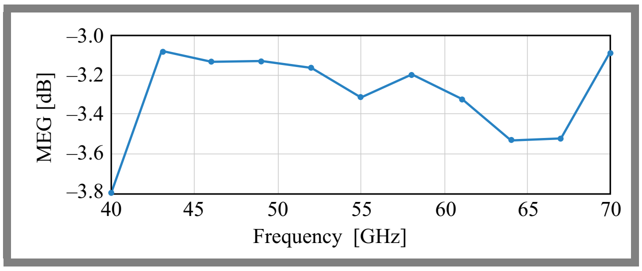

Fig. 10. MEGs of the antenna system.

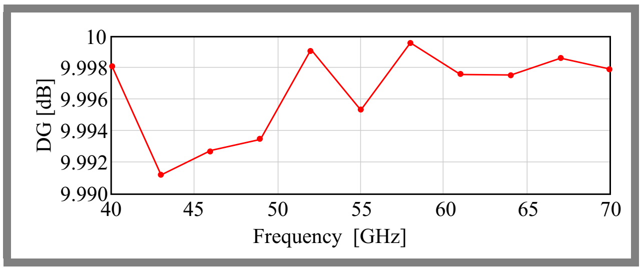

Fig. 11. DG for the proposed MIMO system.

Figure 10 illustrates the MEGs for the four antennas according to Eq. (3), on the far-field radiation, assuming a Gaussian distribution in the elevation direction and a uniform distribution in the azimuth direction. One may notice that the proposed MIMO antenna array meets the condition from Eq. (5) and the MEGs of the quad antennas maintain stable across the frequency band of interest.

The DG value is derived from ECC as [30]:

$$G_{DG} = 10 \times \sqrt{1 - |\rho|^2}\,. \tag{6}$$

A high diversity gain value signifies exceptional performance, while better isolation between the antenna's elements correlates with higher diversity gain values. Figure 11 shows the diversity gain of a MIMO antenna system determined using Eq. (6), which is greater than 9.99 dB across the working band, and thus demonstrates the effective diversity performance of the proposed design.

A comparison between the proposed MIMO array system and other similar recent publications is shown in Tab. 1. The comparison covers several aspects, including bandwidth, efficiency, gain, isolation between antenna elements, ECC, MIMO order, size, and the isolation technique used. The proposed MIMO system features compact dimensions, wide bandwidth, high gain, and decent isolation. The results indicate that the designed MIMO antenna system is a promising candidate for future mmWave devices.

5. Conclusions

This study presents the design of the four-port MIMO antenna array working in the ultra-wideband range from 42.3 to 63.3 GHz. The proposed antenna demonstrates stable radiation properties throughout the operating band, with a peak gain of 7.8 dB. Due to adopting the orthogonality polarization diversity approach, high isolation values of over 24 dB are achieved. Very low ECCs below 0.002 and high DGs over 9.998 dB are obtained as well, ensuring high diversity performance.

Furthermore, optimal MEG values are achieved and the criteria for good performance of the MIMO antenna system are validated by simulations performed using the CST Microwave Studio software. The antenna has achieved the desired performance in terms of gain, efficiency, and radiation properties.

References

[1] M. Shafi *et al.*, "5G: A Tutorial Overview of Standards, Trials, Challenges, Deployment, and Practice", *IEEE Journal on Selected Areas in Communications*, vol. 35, no. 6, pp. 1201–1221, 2017 (`https://doi.org/10.1109/JSAC.2017.2692307`).

[2] M. Agiwal, H. Kwon, S. Park, and H. Jin, "A Survey on 4G-5G Dual Connectivity: Road to 5G Implementation", *IEEE Access*, vol. 9, pp. 16193–16210, 2021 (`https://doi.org/10.1109/ACCESS.2021.3052462`).

[3] J. Cheng, Y. Yang, X. Zou, and Y. Zuo, "5G in Manufacturing: A Literature Review and Future Research", *The International Journal of Advanced Manufacturing Technology*, vol. 131, no. 11, pp. 5637–5659, 2024 (`https://doi.org/10.1007/s00170-022-08990-y`).

[4] B.C. Tedeschini, M. Nicoli, and M.Z. Win, "On the Latent Space of mmWave MIMO Channels for NLOS Identification in 5G-advanced Systems", *IEEE Journal on Selected Areas in Communications*, vol. 41, no. 6, pp. 1655–1669, 2023 (`https://doi.org/10.1109/JSAC.2023.3273769`).

[5] W.A.E. Ali, A.A. Ibrahim, and A.E. Ahmed, "Dual-band Millimeter Wave 2×2 MIMO Slot Antenna with Low Mutual Coupling for 5G Networks", *Wireless Personal Communications*, vol. 129, no. 4, pp. 2959–2976, 2023 (`https://doi.org/10.1007/s11277-023-10267-w`).

[6] W.T. Sethi *et al.*, "Pattern Diversity Based Four-element Dual-band MIMO Patch Antenna for 5G mmWave Communication Networks", *Journal of Infrared, Millimeter, and Terahertz Waves*, vol. 45, no. 5, pp. 521–537, 2024 (`https://doi.org/10.1007/s10762-024-00983-0`).

[7] S. Kumar *et al.*, "Fifth Generation Antennas: A Comprehensive Review of Design and Performance Enhancement Techniques", *IEEE Access*, vol. 8, pp. 163568–163593, 2020 (`https://doi.org/10.1109/ACCESS.2020.3020952`).

[8] A.S. Dixit and S. Kumar, "A Survey of Performance Enhancement Techniques of Antipodal Vivaldi Antenna", *IEEE Access*, vol. 8, pp. 45774–45796, 2020 (`https://doi.org/10.1109/ACCESS.2020.2977167`).

[9] S.F. Farida, P.M. Hadalgi, P.V. Hunagund, and S.R. Ara, "Effect of Substrate Thickness and Permittivity on the Characteristics of Rectangular Microstrip Antenna", *1998 Conference on Precision Electromagnetic Measurements Digest*, Washington, USA, 1998 (`https://doi.org/10.1109/CPEM.1998.700074`).

[10] M.M. Honari, M.S. Ghaffarian, P. Mousavi, and K. Sarabandi, "A Wideband High-gain Planar Corrugated Antenna", *2020 IEEE International Symposium on Antennas and Propagation and North American Radio Science Meeting*, Montreal, Canada, 2020 (`https://doi.org/10.1109/IEEECONF35879.2020.9330020`).

[11] Z.X. Wang and W.B. Dou, "Dielectric Lens Antennas Designed for Millimeter Wave Application", *2006 Joint 31st International Conference on Infrared Millimeter Waves and 14th International Conference on Terahertz Electronics*, Shanghai, China, 2006 (`https://doi.org/10.1109/ICIMW.2006.368584`).

[12] Z. Zhang *et al.*, "Dual-band Focused Transmitarray Antenna for Microwave Measurements", *IEEE Access*, vol. 8, pp. 100337–100345, 2020 (`https://doi.org/10.1109/ACCESS.2020.2998131`).

[13] M.Y. Muhsin, A.J. Salim, and J.K. Ali. "An Eight-element Multi-band MIMO Antenna System for 5G Mobile Terminals", *AIP Conference Proceedings*, vol. 2651, no. 1, 2023 (`https://doi.org/10.1063/5.0105773`).

[14] A. Abdelraheem, H. Elregaily, A.A. Mitkees, and M. Abdalla, "A Hybrid Isolation in Two-element Directive UWB MIMO Antenna", *IETE Journal of Research*, vol. 69, no. 1, pp. 499–508, 2023 (`https://doi.org/10.1080/03772063.2020.1830863`).

[15] M. Khalid *et al.*, "4-Port MIMO Antenna with Defected Ground Structure for 5G Millimeter Wave Applications", *Electronic*s, vol. 9, no. 1, art. no. 71, 2020 (`https://doi.org/10.3390/electronics9010071`).

[16] N. Yoon and C. Seo, "A 28-GHz Wideband 2×2 U-slot Patch Array Antenna", *Journal of Electromagnetic Engineering and Scienc*e, vol. 17, no. 3, pp. 133–137, 2017 (`https://doi.org/10.5515/JKIEES.2017.17.3.133`).

[17] R. Anitha *et al.*, "A Compact Quad Element Slotted Ground Wideband Antenna for MIMO Applications", *IEEE Transactions on Antennas and Propagation*, vol. 64, no. 10, pp. 4550–4553, 2016 (`https://doi.org/10.1109/TAP.2016.2593932`).

[18] C.R. Jetti *et al.*, "Design and Analysis of Modified U-shaped Four Element MIMO Antenna for Dual-band 5G Millimeter Wave Applications", *Micromachines*, vol. 14, no. 8, art. no. 1545, 2023 (`https://doi.org/10.3390/mi14081545`).

[19] D.A. Sehrai *et al.*, "A Novel High Gain Wideband MIMO Antenna for 5G Millimeter Wave Applications", *Electronics*, vol. 9, no. 6, art. no. 1031, 2020 (`https://doi.org/10.3390/electronics9061031`).

[20] E. Al Abbas, M. Ikram, A.T. Mobashsher, and A. Abbosh, "MIMO Antenna System for Multi-band Millimeter-wave 5G and Wideband 4G Mobile Communications", *IEEE Access*, vol. 7, pp. 181916–181923, 2019 (`https://doi.org/10.1109/ACCESS.2019.2958897`).

[21] F.W. Ardianto, F.F. Lanang, S. Renaldy, and T. Yunita, "Design MIMO Antenna with U-Slot Rectangular Patch Array for 5G Applications", *2018 International Symposium on Antennas and Propagation (ISAP)*, Busan, South Korea, 2018.

[22] Y. Rahayu and I.R. Mustofa, "Design of 2×2 MIMO Microstrip Antenna Rectangular Patch Array for 5G Wireless Communication Network", *2017 Progress in Electromagnetics Research Symposium-Fall (PIERS–FALL)*, Singapore, 2017 (`https://doi.org/10.1109/PIERS-FALL.2017.8293591`).

[23] M.K. Ishfaq, T.A. Rahman, Y. Yamada, and K. Sakakibara, "8×8 Phased Series Fed Patch Antenna Array at 28 GHz for 5G Mobile Base Station Antennas", *2017 IEEE-APS Topical Conference on Antennas and Propagation in Wireless Communications (APWC)*, Verona, Italy, 2017 (`https://doi.org/10.1109/APWC.2017.8062268`).

[24] Y. Wang and D. Piao, "A Compact Size Dual-polarized High-gain Resonant Cavity Antenna at 28 GHz", *2017 International Applied Computational Electromagnetics Society Symposium (ACES)*, Suzhou, China, 2017.

[25] A. Thatere, P.L. Zade, and D. Arya, "Bandwidth Enhancement of Microstrip Patch Antenna Using 'U' Slot with Modified Ground Plane", *2015 International Conference on Microwave, Optical and Communication Engineering (ICMOCE)*, Bhubaneswar, India, 2015 (`https://doi.org/10.1109/ICMOCE.2015.7489779`).

[26] I. Rosaline, A. Kumar, P. Upadhyay, and A.H. Murshed, "Four Element MIMO Antenna Systems with Decoupling Lines for High-speed 5G Wireless Data Communication", *International Journal on Antennas and Propagation*, vol. 2022, no. 1, art. no. 9078929, 2022 (`https://doi.org/10.1155/2022/9078929`).

[27] K.S. Sultan and H.H. Abdullah, "Planar UWB MIMO-diversity Antenna with Dual Notch Characteristics", *Progress in Electromagnetics Research C*, vol. 93, pp. 119–129, 2019 (`https://doi.org/10.2528/PIERC19031202`).

[28] R.E.A. Shehata, A. Elboushi, M. Hindy, and H. Elmekati, "Metamaterial Inspired LPDA MIMO array for upper band 5G applications", *International Journal of RF and Microwave Computer-Aided Engineering*, vol. 32, no. 8, art. no. 23212, 2022 (`https://doi.org/10.1002/mmce.23212`).

[29] M.Y. Muhsin, A.J. Salim, and J.K. Ali, "Compact MIMO Antenna Designs Based on Hybrid Fractal Geometry for 5G Smartphone Applications", *Progress in Electromagnetics Research C*, vol. 118, pp. 247–262, 2022 (`https://doi.org/10.2528/PIERC22012808`).

[30] Z.F. Al-Azzawi *et al.*, "Designing Eight-port Antenna Array for Multi-band MIMO Applications in 5G Smartphones", *Journal of Telecommunications and Information Technology*, no. 4, pp. 18–24, 2023 (`https://doi.org/10.26636/jtit.2023.4.1297`).

[31] M.Y. Muhsin *et al.*, "Isolation Techniques in MIMO Antennas for 5G Mobile Devices (Comprehensive Review)", *Radioelectronics and Communications Systems*, vol. 66, no. 6, pp. 263–287, 2023 (`https://doi.org/10.3103/S0735272723040027`).

[32] M. Bilal *et al.*, "High-isolation MIMO Antenna for 5G Millimeter-wave Communication Systems", *Electronics*, vol. 11, no. 6, art. no. 962, 2022 (`https://doi.org/10.3390/electronics11060962`).

[33] H. Elmannai *et al.*, "Design and Characterization of a Meandered V-shaped Antenna Using Characteristics Mode Analysis and its MIMO Configuration for Future mmWave Devices", *AEU – International Journal of Electronics and Communications*, vol. 186, art. no. 155477, 2024 (`https://doi.org/10.1016/j.aeue.2024.155477`).

[34] S. Rahman *et al.*, "Nature Inspired MIMO Antenna System for Future mmWave Technologies", *Micromachines*, vol. 11, no. 12, art. no. 1083, 2020 (`https://doi.org/10.3390/mi11121083`).

Muhannad Y. Muhsin, Ph.D.
Department of Electrical Engineering
https://orcid.org/0000-0003-3937-4467
E-mail: muhannad.y.muhsin@uotechnology.edu.iq
University of Technology – Iraq, Baghdad, Iraq
https://uotechnology.edu.iq

Zainab S. Muqdad, M.Sc.
Electrical Engineering Department
https://orcid.org/0009-0003-1342-7994
E-mail: zainab.salam@uomustansiriyah.edu.iq
Mustansiriyah University, Baghdad, Iraq
https://uomustansiriyah.edu.iq

Asaad H. Sahar, Ph.D.
Electronics and Communication Engineering Department
https://orcid.org/0000-0003-3655-0162
E-mail: asaad.h@coeng.uobaghdad.edu.iq
University of Baghdad, Baghdad, Iraq
https://en.uobaghdad.edu.iq

Zainab F. Mohammad, M.Sc.
Communication Engineering Department
https://orcid.org/0000-0002-1627-751X
E-mail: zainab.f.mohammad@uotechnology.edu.iq
University of Technology – Iraq, Baghdad, Iraq
https://uotechnology.edu.iq

Hussam AL-Saedi, Ph.D.
Communication Engineering Department
https://orcid.org/0000-0002-2029-7361
E-mail: hussam.h.ali@uotechnology.edu.iq
University of Technology – Iraq, Baghdad, Iraq
https://uotechnology.edu.iq